

Structured Energy Distribution and Coherent AC Transport in Mesoscopic Wires

A. V. Shytov

Lyman Laboratory, Harvard University, Cambridge, MA 02138

L. D. Landau Institute for Theoretical Physics, Kosygina str., 2, Moscow 117934, Russia

Electron energy distribution in a mesoscopic AC-driven diffusive wire generally is not characterized by an effective temperature. At low temperatures, the distribution has a form of a multi-step staircase, with the step width equal to the field energy quantum. Analytic results for the field frequency high and low compared to Thouless energy are presented, while the intermediate frequency regime is analyzed numerically. Manifestations in the tunneling spectroscopy and noise measurements are discussed.

In mesoscopic micron-size wires, at low temperatures, the electron-phonon energy relaxation time τ_{e-ph} can exceed the time τ_D of diffusion across the wire [1]. In this regime, when electron cooling is primarily diffusive, the system temperature has a very short thermal response time to microwave radiation, determined mainly by the diffusion time τ_D . This makes such diffusion-cooled wires an excellent system for fast bolometric detection of terahertz radiation [2,3].

When the wire dimension, or electron temperature T_e , decreases further, one arrives at the situation, demonstrated in Saclay experiments [4,5], when the electron-electron energy relaxation is longer than the diffusion time τ_D . When this happens, the electron dynamics can be considered as purely elastic. Importantly, the effect of microwave field on electron energy distribution in this case *is not described by an effective temperature*. Since the energy of the field is absorbed in discrete quanta $\hbar\omega$, and there is not enough time to redistribute it between electrons while they move around in the wire, one expects a staircase-like energy distribution to emerge, consisting of $\hbar\omega$ wide steps. The steps will be pronounced when the temperature of electrons is below $\hbar\omega$.

In this article, our goal is to develop a general approach that allows to analyze such a situation. We shall focus on the regime when the field frequency is small compared to the elastic scattering rate due to disorder, which corresponds to the experimental situation [2,3,5]. Since in this case the transport is diffusive on the field oscillation time scale $2\pi/\omega$, the system can be described by momentum-averaged Greens functions, similar to Usadel theory of disordered superconductors. We develop a general framework to analyze the energy distribution, using Keldysh Greens functions, and then apply it to obtain analytic results in the two regimes, when the field frequency is small and large compared to Thouless energy $E_T = \hbar/\tau_D$. In the intermediate regime, $\omega\tau_D \sim 1$, we present numerical results.

The energy distribution of this form can be probed by tunneling spectroscopy, similar to the DC transport situation, when a double step structure arises from mixing

of the lead Fermi functions at nonequal chemical potentials [4]. Another manifestation we consider is in the shot noise, where the structure of the energy distribution affects the noise power.

Before discussing the AC mesoscopic transport problem, let us recall, for comparison, the basic facts about the DC transport. At low temperatures, when electron energy relaxation is slow, charge transport is mainly controlled by elastic scattering due to disorder. At high conductance, when the localization effects are negligible, the sample properties can be fully described by a scattering matrix. All the statistics of transport in this case are controlled by a single parameter, the sample conductance (see review [6]).

In the DC regime, the energy gained by an electron moving in a stationary electric field depends only on the total electron position displacement and is independent of the trajectory shape. As a result, the electron energy distribution in a wire carrying a DC current does not depend on microscopic parameters and is fully determined by the external voltage and the wire geometry. The energy distribution in the DC case was explored by Nagaev [7,8], who obtained a position-dependent mixture of two Fermi functions in the limit of slow energy relaxation, and a single Fermi distribution with position-dependent effective temperature in the limit of fast relaxation, and studied the effect on the shot noise. More recently, Nagaev [9] has shown that the time-dependent current fluctuations of all orders can be expressed through the nonequilibrium electron energy distribution.

In the AC case, in contrast, the energy gained by an electron depends on its whole trajectory. The AC transport can thus reveal additional information about phase-sensitive effects in electron dynamics. It was pointed out by Lesovik and Levitov [10] that even a slowly varying AC field leads to a new transport effect, photon-assisted noise, observed by Schoelkopf et al. [11] and recently by Glattli et al. [12]. The photon-assisted effects can be expected to become more drastic and interesting when the field frequency is comparable to Thouless energy.

In this paper, a semiclassical treatment of ac trans-

port in mesoscopic wire is adopted. In a time-dependent external field, the uncertainty principle restricts the ability to measure the energy of an electron as a function of time, and the time-dependent energy distribution function should be carefully defined. In this work, we employ the Wigner distribution function and show that in the presence of an AC field, the time-averaged electron distribution consists of $\hbar\omega$ steps. Subsequently, we discuss the manifestation of such distribution in tunneling spectroscopy [4] and in noise.

Let us now turn to the analysis of the energy distribution. Non-equilibrium electrons in a diffusive conductor can be fully described by the retarded and advanced Greens function $G^R(t, t', \mathbf{r}, \mathbf{r}')$ and $G^A(t, t', \mathbf{r}, \mathbf{r}')$, and Keldysh function $F(t, t', \mathbf{r}, \mathbf{r}')$ defined in [14]. In a diffusive conductor, many quantities can be calculated from momentum-averaged Greens function (i.e., taken at equal points in space, $\mathbf{r} = \mathbf{r}'$). Then, since for noninteracting electrons, the functions $G^R(t, t')$ and $G^A(t, t')$ are independent of the external fields, any quantity of interest can be expressed entirely in terms of the Keldysh function $F(t, t', \mathbf{r})$.

The Keldysh function $F(t_1, t_2, \mathbf{r})$ contains information about both energy distribution and the single-particle density of states. To separate the density of states, we introduce the function $f(t_1, t_2, \mathbf{r})$ (see, *e.g.*, [17]),

$$F = G_R - G_A - 2G_R * f + 2f * G_A, \quad (1)$$

where $f * g$ stands for the convolution

$$(f * g)(t, t') = \int_{-\infty}^{\infty} f(t, t'')g(t'', t')dt''. \quad (2)$$

Then, the details of the electron spectrum are hidden in the Green's functions $G^{R,A}(t_1, t_2)$, while the function $f(t_1, t_2, \mathbf{r})$ depends only on the energy distribution.

Consider a disordered wire of length L with diffusion coefficient D , connected to the leads which serve as a source of equilibrium electrons. The wire is subject to electric field which we describe as an external vector potential

$$A_x(t) = (cU/L\omega) \cos \omega t, \quad (3)$$

where U is the amplitude of voltage across the wire, and ω is the frequency of the external field. At frequencies low compared to the plasma frequency and Maxwell relaxation rate, the longitudinal component of electric field is screened. Thus, the electric field can be described through the vector potential $\mathbf{A}(\mathbf{r}, t)$ only.

The equal point Keldysh function $f(t_1, t_2, \mathbf{r})$ satisfies the two-time diffusion equation [15–17]

$$\left\{ \frac{\partial}{\partial t_+} + D \left[-i\nabla - \frac{e}{c} \mathbf{A}(t_1, t_2, \mathbf{r}) \right]^2 \right\} f(t_1, t_2, \mathbf{r}) = 0, \quad (4)$$

with $t_+ = (t_1 + t_2)/2$ and $\mathbf{A}(t_1, t_2, \mathbf{r}) = \mathbf{A}(t_1, \mathbf{r}) - \mathbf{A}(t_2, \mathbf{r})$. This equation has to be supplemented with the boundary condition at the leads:

$$f(t_1, t_2, x = 0) = f(t_1, t_2, x = L) = f_F(t_1 - t_2), \quad (5)$$

where $f_F(t_1 - t_2)$ is the Keldysh function of an equilibrium Fermi gas.

It is convenient to rewrite the vector potential difference as

$$\begin{aligned} \mathcal{A}_x(t_1, t_2, x) &= A_x \left(t + \frac{\tau}{2} \right) - A_x \left(t - \frac{\tau}{2} \right) \\ &= 2 \frac{cU}{L\omega} \sin \omega t \sin \frac{\omega\tau}{2}, \quad \tau = t_1 - t_2. \end{aligned} \quad (6)$$

Passing to the Wigner representation, we replace τ by $i\partial_\epsilon$. Now, using the general operator relation

$$\exp \left(a \frac{\partial}{\partial \epsilon} \right) \Phi(\epsilon) = \Phi(\epsilon + a), \quad (7)$$

valid for an arbitrary function $\Phi(\epsilon)$, one arrives at

$$\mathcal{A}_x(t_1, t_2, x) = -\frac{icU}{L} \sin(\omega t) \mathcal{D}_\omega, \quad (8)$$

where \mathcal{D}_ω is a finite difference operator

$$\mathcal{D}_\omega f(\epsilon) = \frac{f(\epsilon + \omega/2) - f(\epsilon - \omega/2)}{\omega}. \quad (9)$$

Next, we perform variable rescaling,

$$t \rightarrow t\omega, \quad x \rightarrow x/L, \quad \epsilon \rightarrow \epsilon/eU \quad (10)$$

i.e., measure time in the units of ω^{-1} , x in the units of L , and energy in the units of eU . After that, the equation for the distribution function becomes

$$\left[\frac{\partial}{\partial t} - \frac{1}{\omega\tau_D} \left(\frac{\partial}{\partial x} - \sin t \mathcal{D}_\omega \right)^2 \right] f(t, \epsilon, x) = 0, \quad (11)$$

where $\tau_D = L^2/D$ is the time of diffusion across the wire.

For a wire connected to the leads, the boundary condition to the Eq. (11) takes the form

$$f(t, \epsilon, x = 0) = f(t, \epsilon, x = 1) = n_F(\epsilon), \quad (12)$$

where $n_F(\epsilon)$ is a Fermi distribution. For a wire that has been in equilibrium with the leads before the field was turned on, the initial condition is

$$f(t = 0, \epsilon, x) = n_F(\epsilon) \quad (13)$$

for any x .

Note that the operator \mathcal{D}_ω in Eq. (11) relates the values of the distribution function $f(\epsilon)$ only for the energies that differ by $\pm \frac{1}{2}\hbar\omega$. Thus, at zero temperature the singularity at $\epsilon = 0$ in the boundary condition (12) propagates to the energies $\epsilon_n = \frac{1}{2}n\hbar\omega$. Also, since the Fermi

distribution $n_F(\epsilon)$ is flat for $\epsilon < 0$ and $\epsilon > 0$, the distribution function is also flat for $\epsilon_n < \epsilon < \epsilon_{n+1}$. Thus, the profile of $f(t, \epsilon, x)$ is a series of steps at energies $n\hbar\omega/2$. In fact, only the even steps ($\epsilon_{2n} = n\hbar\omega$) corresponding to absorption of individual field quanta, survive after averaging over time.

For slow field, $\omega\tau_D \ll 1$, one may neglect the time derivative in Eq. (11). The solution to Eq. (11) is then

$$f(t, \epsilon, x) = [(1-x) \exp(x\mathcal{D}_\omega \sin t) + x \exp((x-1)\mathcal{D}_\omega \sin t)] n_F(\epsilon). \quad (14)$$

The exponent of the operator \mathcal{D}_ω can be found using Fourier transform in the energy domain. The result is

$$\exp(\alpha\mathcal{D}_\omega)\Phi(\epsilon) = \sum_{n=-\infty}^{\infty} \Phi(\epsilon - n\omega/2) J_n(2\alpha/\omega), \quad (15)$$

where $\Phi(\epsilon)$ is an arbitrary function, $J_n(x)$ is the Bessel function of n th order, and the sum runs over all integer n . As we discuss below, one is mostly interested in the time-averaged distribution function, because it can be directly measured by tunneling spectroscopy. Substituting Eq. (15) into Eq. (14), and using the formula $\overline{J_{2k}(2a \sin t)} = J_k^2(a)$ to average over t , one finds, with the original units restored,

$$\bar{f}_0(\epsilon, x) = \left(1 - \frac{x}{L}\right) F_0(\epsilon, x) + \frac{x}{L} F_0(\epsilon, L-x), \quad (16)$$

where

$$F_0(\epsilon, x) = \sum_{k>\epsilon/\omega}^{\infty} J_k^2(\tilde{u}), \quad \tilde{u} = \frac{x e U}{L \hbar \omega}. \quad (17)$$

(We mention that an expression of the form similar to (14) for nonaveraged function f was used by Altshuler *et al.* in the calculation of time-dependent noise [18].)

To interpret the result (16), note that the work performed by a slow field on electrons that travel a distance x along the wire, is $\epsilon U x/L$. Then, according to [19], the probability of absorbing n field quanta is $J_n^2(\tilde{u})$. The factor $(1-x/L)$ in Eq. (16) is the number of the electrons at cross-section x coming from the left lead (cf. [7]). The second term in Eq. (16) describes electrons that come from the right lead.

In the limit $\omega \ll eU$, one may use the asymptotic form of the Bessel function at $x/\omega \sim n \gg 1$, which gives

$$F_0(\epsilon, x) = \begin{cases} 1, & \tilde{\epsilon} < -1 \\ \frac{1}{\pi} \cos^{-1} \tilde{\epsilon}, & |\tilde{\epsilon}| < 1 \\ 0, & \tilde{\epsilon} > 1 \end{cases}, \quad \tilde{\epsilon} = \frac{L\epsilon}{xeU}, \quad (18)$$

This result can also be derived by time averaging the two-step distribution found in [7] over the time-dependent voltage difference.

For fast field, $\omega\tau_D \gg 1$, the first term in Eq. (11) is the most important. Thus, the electron distribution is

almost time-independent. (The time-dependent part of $f(t, \epsilon, x)$ is proportional to $(\omega\tau_D)^{-1}$.) Projecting out the time-dependent part of the distribution function, i.e., averaging the Eq. (11) over field period, one finds the equation for the time-averaged electron distribution:

$$\left[\frac{\partial^2}{\partial x^2} + \frac{1}{2} \mathcal{D}_\omega^2 \right] \bar{f}(\epsilon, x) = 0. \quad (19)$$

Using Fourier transform with respect to energy, one can find the solution of Eq. (19) in a closed integral form. It is more instructive, however, to solve this equation in the limit $\hbar\omega \ll eU$, where one can replace \mathcal{D}_ω by ∂_ϵ . This brings Eq. (19) to the form of a Laplace's equation in the two-dimensional strip $0 < x < 1$, $-\infty < \epsilon < \infty$. Using the function

$$w = \exp(\pi i(x + i\sqrt{2}\epsilon)), \quad (20)$$

one can conformally map this strip onto half-plane $\text{Im } w > 0$. The boundary condition (12) on the line $\text{Im } w = 0$ is, for $T_e = 0$:

$$\bar{f}_\infty(w) = \begin{cases} 0, & |\text{Re } w| < 1, \\ 1, & |\text{Re } w| > 1 \end{cases}. \quad (21)$$

This boundary value problem is solved by an imaginary part of the analytic function

$$\bar{f}_\infty(w) = \text{Im} \frac{1}{\pi} \log \left(\frac{1-w}{1+w} \right) \quad (22)$$

Restoring the original dimensional units, one obtains

$$\bar{f}_\infty(\epsilon, x) = \frac{1}{\pi} \cotan^{-1} \left(\frac{\sinh(\pi\sqrt{2}\epsilon/eU)}{\sin(\pi x/L)} \right) \quad (23)$$

Unlike the low frequency solution (16) with $F_0(\epsilon, x)$ given by Eq. (18), the high frequency distribution Eq. (23) is non-zero at large ϵ . Physically, this difference is due to the fact that maximal energy that can be gained from the field is given by the bias amplitude eU only in the DC regime. In contrast, in a varying field, there is a finite probability that electron diffuses several times back and forth in phase with the field, thus gaining energy that exceeds eU .

Eqs. (16), (18) and (23) are correct in the limit $\omega \ll eU$. For finite values of ω/eU these results approximate the average profile of the step-like electron distribution. To obtain the distribution at intermediate frequencies, $\omega\tau_D \simeq 1$, Eq. (11) was solved numerically for different values of eU/ω . The results are shown on Fig. 1. From that figure one may see that a crossover from the low-frequency behavior to the high-frequency behavior occurs at $\omega\tau_D \sim 100$. To understand the origin of this large numerical factor, note that the electron distribution relaxes at $t \rightarrow \infty$, according to the diffusion equation, as $\exp(-\mu t)$, where μ is the lowest non-zero eigenvalue of

a diffusion operator: $\mu = \pi^2/\tau_D$. Assuming that the crossover occurs when the relaxation time is of order of field period, $2\pi/\omega$, one finds $\omega\tau_D \sim 2\pi^3 \approx 60$, in a qualitative agreement with the numerical data.

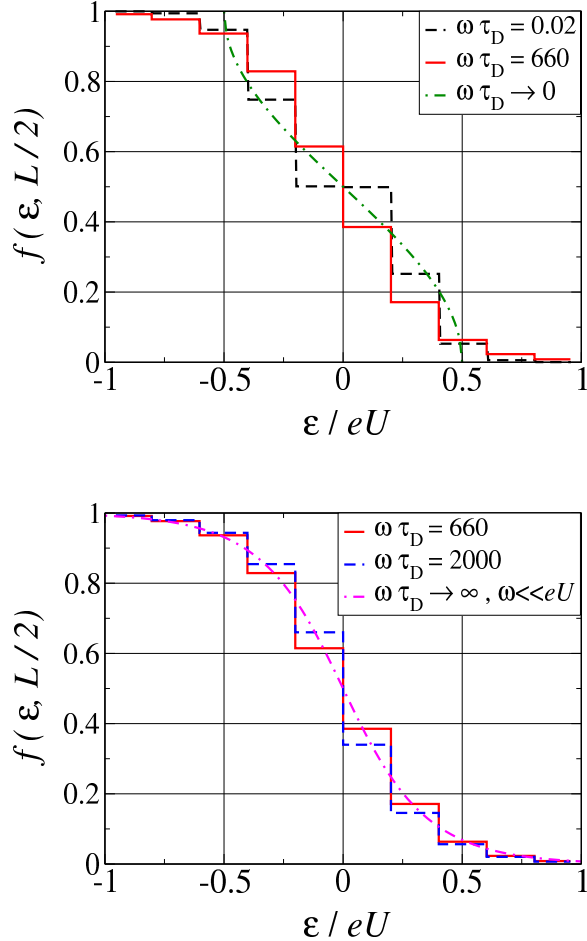


FIG. 1. The energy distribution at the wire midpoint $x = L/2$, calculated numerically for $\hbar\omega = 0.2eU$, for different values of $\omega\tau_D$. The height of the $\hbar\omega$ steps is a function of external voltage and other system parameters. The envelope of the staircase structure changes as the frequency of the field increases, demonstrating a crossover from the slow to the fast field regime.

To characterize the electron distribution, one may compute its second moment, or shot noise. For low frequencies, the answer can be derived just by averaging over time the well known result for the shot noise [7]:

$$S_0 = \frac{2}{3}eG\overline{|U(t)|} = \frac{4}{3\pi}eGU \approx 0.424eGU, \quad (24)$$

where G is a conductance of the wire. For high frequencies, one may neglect the time dependence of the distribution function and compute the noise as [7]

$$S_\infty = 4eGU \int_{-\infty}^{\infty} \int_0^1 d\epsilon dx \bar{f}_\infty(\epsilon, x)(1 - \bar{f}_\infty(\epsilon, x)). \quad (25)$$

Evaluating the integral, one arrives at

$$S_\infty = \frac{21\sqrt{2}}{2\pi^3} \zeta(3) eGU \approx 0.575 eGU, \quad (26)$$

where $\zeta(3)$ is Riemann zeta-function. The value given by Eq. (26) is higher than that in Eq. (24), because of the contributions of high energy tails of the distribution (23).

The electron distribution can also be probed by superimposing a DC voltage U_{dc} , which splits every step into two, separated by eU_{dc} . When this splitting becomes equal to $\hbar\omega$, the “resonance” between two steps leads to a singularity in the shot noise and higher current moments, predicted for short wires in [10] and observed in [11].

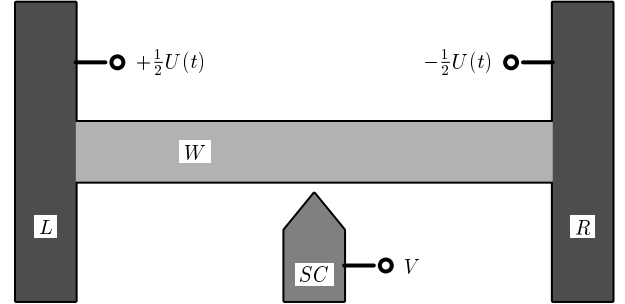


FIG. 2. Schematic representation of the measurement [4], in which the energy distribution in a mesoscopic wire (W) is probed by a NS tunneling junction between the wire and the superconducting probe (SC). By changing voltage V across the junction, one may scan the energy of tunneling electrons. AC voltage $U(t)$ applied between the leads (L and R), creates a nonequilibrium energy distribution in the wire.

Finally, we discuss how the structure in the energy distribution considered above will manifest itself in the tunneling spectroscopy measurement [4,5]. In this setup, a short segment of the sample at point \mathbf{r}_0 is connected to a metallic probe by a tunneling junction (see Fig. 2). The tunneling density of states of the probe must contain a sharp feature that serves as a “pointer”, allowing to probe electron distribution. (In [4], the probe was a superconductor, and the BCS square root singularity near the superconducting gap was used.) Applying the probing voltage V to the junction, allows one to scan the energy domain. The electron energy distribution in the sample is then extracted from the $I - V$ curve of the tunnel junction.

To derive the relation between the tunneling current and the energy distribution in a nonequilibrium system, one may use the standard tunneling Hamiltonian

$$\hat{H}_T(t) = \sum_{\mathbf{p}, \mathbf{k}} T_{\mathbf{p}, \mathbf{k}} a_{\mathbf{p}}^{\dagger}(t) b_{\mathbf{k}}(t) + \text{h.c.} \quad (27)$$

(see, e.g., [13]). Here $a_{\mathbf{p}}(t)$ and $b_{\mathbf{k}}(t)$ are electron operators of the sample and the probe. The tunneling current operator in this formalism is

$$\hat{I}_T(t) = i \sum_{\mathbf{p}, \mathbf{k}} T_{\mathbf{p}, \mathbf{k}} a_{\mathbf{p}}^{\dagger}(t) b_{\mathbf{k}}(t) + \text{h.c.} . \quad (28)$$

The average tunneling current $I(t)$ can be found from Kubo formula:

$$I(t) = i \int_{-\infty}^t dt' \left\langle \left[\hat{H}_T(t'), \hat{I}_T(t) \right] \right\rangle . \quad (29)$$

Using the Keldysh approach [14], one may express the tunneling current $I(t)$ in terms of retarded and advanced Green's function $G^{R(A)}(t_1, t_2)$ and Keldysh function $F(t_1, t_2)$ defined in [14]:

$$I(t) \propto \text{Re} \left[F_s^R * G_p^R - F_p * G_s^R \right] \Big|_{t'=t} \quad (30)$$

(subscripts s and p denote the sample and the probe, all functions are taken at space point \mathbf{r}_0 , where the tunneling occurs). The star denotes the convolution defined by Eq. (2).

It is now convenient to express all quantities in frequency domain. In the noninteracting system, the functions $G^{R,A}(t_1, t_2)$ depend only on the difference of their arguments $t_1 - t_2$. Their Fourier components are related through the Kramers-Kronig relation to the density of states $\nu(\omega)$ defined by

$$\pi \nu(\omega) = \text{Im} G^R(\omega) = -\text{Im} G^A(\omega) . \quad (31)$$

The function $f(t_1, t_2)$ in general depends on both arguments. We define its Fourier transform as

$$f_{\omega}(\epsilon) = \int dt dt' e^{i\epsilon(t-t')} e^{i\omega(t+t')/2} f(t, t') . \quad (32)$$

Thus, $f_{\omega}(\epsilon)$ is a Fourier transform of the Wigner distribution

$$f(\epsilon, t) = \int f(t + \tau/2, t - \tau/2) e^{i\epsilon\tau} d\tau . \quad (33)$$

Then, the Fourier components of the tunneling current (30) are given by

$$I_{\omega} \propto \int_{-\infty}^{\infty} d\epsilon \nu_s \left(\epsilon + \frac{\omega}{2} \right) \nu_p \left(\epsilon + \frac{\omega}{2} \right) [f_{s,\omega}(\epsilon) - f_{p,\omega}(\epsilon)] . \quad (34)$$

In an equilibrium system, the function $f_{\omega}(\epsilon)$ coincides with the Fermi distribution [14]: $f_{\omega}(\epsilon) = 2\pi n_F(\epsilon) \delta(\omega)$. Thus, $f(\epsilon, t)$ can be identified as the conventional energy distribution function.

The probing voltage V simply shifts energy levels of the probe by eV . Thus, the tunneling current is:

$$I_{\omega}(eV) \propto \int d\epsilon \nu_s \left(\epsilon + \frac{\omega}{2} \right) \nu_p \left(\epsilon + \frac{\omega}{2} + eV \right) \times [f_{s,\omega}(\epsilon) - f_{p,\omega}(\epsilon + eV)] . \quad (35)$$

Eq. (35) shows that in general, the relation between the tunneling current and energy distribution function is not straightforward, because all factors in (35) depend on the current frequency ω . (One cannot extract the energy distribution from tunneling measurements if both $\nu_s(\epsilon)$ and $\nu_p(\epsilon)$ are flat.) The ω -dependence of the product $\nu_s(\epsilon + \omega/2) \nu_p(\epsilon + \omega/2 + eV)$ leads to a non-local relation between energy distribution and tunneling current. This non-locality does not allow to measure Wigner function directly. However, for $\omega = 0$, the average tunneling current is proportional to the average electron distribution:

$$\bar{I}(eV) \propto \int d\epsilon \nu_s(\epsilon) \nu_p(\epsilon + eV) [\bar{f}_s(\epsilon) - \bar{f}_p(\epsilon + eV)] , \quad (36)$$

where the bar denotes averaging over one field period. Thus, the tunneling spectroscopy technique of [4] allows to measure directly the time-averaged electron energy distribution.

The effect of finite temperature can be understood as follows. At finite electron temperature T_e , the singularity in the boundary condition (12) is smeared. The resulting smearing of the step-like structure is negligible for $\hbar\omega > T_e$. For a wire length $L = 1 \mu\text{m}$, the electron mean free path $l = 10 \text{nm}$, and Fermi velocity $v_F = 10^7 \text{m/s}$ the diffusion time is $\tau_D = L^2/v_F l = 10^{-11} \text{s}$. The fast field regime occurs for $\omega\tau_D > 100$, *i.e.*, for the frequencies $f = \omega/2\pi > 1 \text{THz}$. The optimal voltage amplitude is of the order of $10\hbar\omega$, *i.e.* $V \sim 50 \text{mV}$. The temperature must be less than $\hbar\omega/k_B$, *i.e.*, $T < 10 \text{K}$. These conditions appear realistic, and can be fulfilled in an experiment.

The simple theory presented in this paper does not take into account the effect of non-equilibrium density fluctuations in the wire on the density of states of the superconducting probe through long-range Coulomb forces [20]. The treatment of this effect for an AC field is beyond the scope of this paper. However, since the non-equilibrium fluctuations are also due to periodic field, the resulting tunneling current will also have singularities at quantization energies $n\hbar\omega$, although the shape of these singularities may differ from simple steps.

To summarize, the energy distribution of a mesoscopic AC-driven wire is not described by an effective temperature. The most interesting feature of the electron distribution is the $\hbar\omega$ steps due to quantization of absorbed energy. Those steps are present at the external field frequencies larger than electron temperature. The calculated envelope in the fast-field regime distribution is qualitatively different from that of the slow-field regime.

Experimental manifestations of these effects experimentally are discussed.

I am grateful to D. Esteve, H. Pothier, M. V. Feigel'man, L. S. Levitov and E. G. Mishchenko for stimulating discussions. This research was supported by the Russian Ministry of Science under the program "Physics of quantum computing," by RFBR grant 98-02-19252 and NSF grant PHY99-07949.

-
- [1] D. E. Prober, Appl. Phys. Lett., **62**, 2119 (1993);
 - [2] A. Skalare, W. R. McGrath, B. Bumble, H. G. LeDuc, P. J. Burke, A. A. Verheijen, R. J. Schoelkopf, and D. E. Prober, Appl. Phys. Lett., **68**, 1558 (1996);
 - [3] B. S. Karasik, M. C. Gaidis, W. R. McGrath, B. Bumble, and H. G. LeDuc, Appl. Phys. Lett., **71**, 1567 (1997)
 - [4] H. Pothier, S. Gueron, N. O. Birge, D. Esteve, M. H. Devoret, Phys. Rev. Lett., **79**, 3490 (1997); Z. Phys. B – Condensed Matter, **104** (1), 178 (1997)
 - [5] A. B. Gougam, F. Pierre, H. Pothier, D. Esteve, N. O. Birge, J. Low Temp. Phys. **118**, 447 (2000); F. Pierre, H. Pothier, D. Esteve, M. H. Devoret, J. Low Temp. Phys. **118**, 437-445; A. Anthore, F. Pierre, H. Pothier, D. Esteve, Phys. Rev. Lett. **90**, 076806 (2003)
 - [6] C. W. J. Beenakker, Rev. Mod. Phys. **69**, 731 (1997).
 - [7] K. E. Nagaev, Phys. Lett. A **169**, 103 (1992)
 - [8] K. E. Nagaev, Phys. Rev. B **52**, 4740 (1995)
 - [9] K. E. Nagaev, Phys. Rev. B, **66** 075334 (2002)
 - [10] G. B. Lesovik and L. S. Levitov, Phys. Rev. Lett., **72**, 538 (1994)
 - [11] R. J. Schoelkopf *et al*, Phys. Rev. Lett., **80**, 2437 (1997)
 - [12] L.-H. Reydellet, P. Roche, D. C. Glattli, B. Etienne, Y. Jin, cond-mat/0206514
 - [13] G. D. Mahan, *Many Particle Physics*, Sec. 4.4, Plenum Press, NY (1990)
 - [14] L. V. Keldysh, Zh. Eksp. Theor Fiz, **47**, 1515 (1964) [JETP **20**, 1018]
 - [15] A. I. Larkin and D. E. Khmel'nitskii, Zh. Eksp. Theor. Fiz **91**, 1815 (1986) [JETP **64**, 1075]
 - [16] B. L. Altshuler, Zh. Eksp. Theor. Fiz. **75**, 1330 (1978) [JETP **48**, 670]
 - [17] B. L. Altshuler and A. G. Aronov, in *Electron-Electron interactions in disordered conductors*, eds. A. L. Efros and M. Pollak (Elsevier, Amsterdam, 1985)
 - [18] B. L. Altshuler, L. S. Levitov, and A. Yu. Yakovets, JETP Lett. **59**, 857 (1994)
 - [19] P. K. Tien and J. P. Gordon, Phys. Rev. **129**, 647 (1963)
 - [20] B. N. Narozhny, I. L. Aleiner, and B. L. Altshuler, Phys. Rev. B **60**, 7213 (1999)